Journal of Southeast University (English Edition) Vol. 40, No. 4, pp. 346 - 354 Dec. 2024 ISSN 1003—7985

Optimal intensity measures for longitudinal seismic response of tunnels

Zhao Xu[1] Yang Yujie[1] Huang Jingqi[2] Zhao Mi[1] Cao Shengtao[3]

([1]Key Laboratory of Urban Security and Disaster Engineering of Ministry of Education, Beijing University of Technology, Beijing 100124, China)

([2]School of Civil and Resource Engineering, University of Science and Technology Beijing, Beijing 100083, China)

([3]Guangzhou Yingli Technology Co., Ltd., Guangzhou, 510700, China)

Abstract: To study the ground motion intensity measures (IMs) suitable for the design of seismic performance with a focus on longitudinal resistance in tunnel structures, 21 different seismic intensity parameters are selected for nonlinear calculation and analysis of tunnel structures, in order to determine the optimal IM for the longitudinal seismic performance of tunnel structures under different site conditions. An improved nonlinear beam-spring model is developed to calculate the longitudinal seismic response of tunnels. The PQ-Fiber model is used to simulate the longitudinal nonlinear behavior of tunnel structures and the tangential interactions between the tunnel and the soil is realized by load in the form of moment. Five different site types are considered and 21 IMs is evaluated against four criteria: effectiveness, practicality, usefulness, and sufficiency. The results indicate that the optimal IMs are significantly influenced by the site conditions. Specifically, sustained maximum velocity (V_{SM}) emerges as the optimal IM for circular tunnels in soft soil conditions (Case Ⅰ sites), peak ground velocity (V_{PG}) is best suited for Case Ⅱ sites, sustained maximum acceleration (A_{SM}) is ideal for both Case Ⅲ and Case Ⅴ sites, and peak ground acceleration (A_{PG}) for Case Ⅳ sites. As site conditions transition from Case Ⅰ to Case Ⅴ, from soft to hard, the applicability of acceleration-type intensity parameters gradually decreases, while the applicability of velocity-type intensity parameters gradually increases.

Key words: seismic intensity measures; tunnel longitudinal direction; probabilistic seismic demand model; soil-tunnel interaction; improved ground-beam model

DOI: 10.3969/j.issn.1003-7985.2024.04.003

Tunnels are vital components of urban lifeline projects and essential elements of modern metropolitan transportation networks. Despite tunnels historically being considered more seismically resilient than aboveground structures[1], numerous strong seismic events worldwide over the last few decades have inflicted significant damage on them. These seismic damage cases have shattered the traditional perception of tunnels' seismic resilience, emphasizing the urgent need for enhanced seismic safety considerations in the design of underground structures. Therefore, investigating the seismic response behavior and evaluating their seismic performance have become critical[2-6].

Determining the optimal intensity measure (IM) is a significant challenge in earthquake engineering research, aiming to accurately represent the seismic ground motion intensity and reduce the variability in structural responses[7]. Unlike aboveground structures, the seismic response of tunnels and other underground structures is mainly affected by seismic-induced ground deformation and the soil-structure interactions rather than the structure's own inertia. Accordingly, determining the optimal IM for tunnel structures demands meticulous attention. Chen et al.[8] evaluated IMs in mountain tunnels and found that velocity-type IMs demonstrate the highest correlation. Zhang et al.'s[9] analysis highlighted sustained maximum acceleration as the optimal IM among 20 commonly used ones for evaluating damage in circular tunnels. The above studies, however, have mainly focused on the seismic IMs for cross-sectional aspects of tunnels. The longitudinal dynamics of tunnel structures, including their susceptibility to longitudinal bending and axial compression induced by non-uniform seismic wave excitation, have received poor attention[10]. Therefore, seismic responses in the longitudinal direction of tunnel structures should receive equal attention as those in the transverse direction. This should be further applied in assessing the optimal IM for longitudinal tunnel structures. Yet, studies addressing the optimal IMs for longitudinal seismic response in tunnels have been scarce.

This study focuses on the optimal IMs for the longitudinal probabilistic seismic demand model of continuous tunnels constructed using the drilling and blasting method. Based on the calculated tunnel seismic responses, 21 IMs

Received 2024-03-02, **Revised** 2024-04-02.

Biographies: Zhao Xu (1976—), female, docotor, associate professor; Zhao Mi (corresponding author), male, docotor, professor, zhaomi@bjut.edu.cn.

Foundation items: National Key Research and Development Program of China (No. 2022YFC3004300), the National Natural Science Foundation of China (No. 52378475).

Citation: Zhao Xu, Yang Yujie, Huang Jingqi, et al. Optimal intensity measures for longitudinal seismic response of tunnels[J]. Journal of Southeast University (English Edition), 2024, 40(4): 346 - 354. DOI: 10.3969/j.issn.1003-7985.2024.04.003.

were examined using selection criteria such as correlation, efficiency, practicality, and proficiency. The peak bending moment ratio was selected as the engineering demand parameter (DM). The seismic response of the tunnel in the longitudinal direction was calculated using an improved nonlinear beam-spring model. In this model, the PQ-Fiber beam model is employed to simulate the nonlinear behavior in the longitudinal direction of the tunnel, and the torsional moment is considered to account for the tangential interactions between the tunnel and the soil. The study encompassed five different site classes, corresponding to the site categories specified in the Chinese code for seismic design of urban rail transit structures. Through a thorough analysis of the results, the optimal IMs for the longitudinal response of tunnels were recommended.

1 Selection of Intensity Measures and Evaluation Criteria

1.1 Section of intensity measures

In this study, 21 seismic intensity parameters were selected[11-12]. These IMs can be broadly classified into two types: 1) IMs that consider only seismic motion information. These IMs can be directly obtained from seismic records, such as peak ground acceleration (A_{PG}), peak ground velocity (V_{PG}), and peak ground displacement (D_{PG}). 2) IMs related to structural characteristics. These IMs need to be determined indirectly through computer-aided analysis.

1) Peak ground acceleration

$$A_{PG} = \max | a(t) | \tag{1}$$

2) Sustained maximum acceleration (A_{SM}): Third largest peak in acceleration time history.

3) Arias intensity

$$I_A = \frac{\pi}{2g}\int_0^{t_f} a^2(t)\,\mathrm{d}t \tag{2}$$

4) Cumulative absolute velocity

$$I_{CAV} = \int_0^{t_f} | a(t) | \,\mathrm{d}t \tag{3}$$

5) Acceleration root mean square (RMS)

$$a_{rms} = \sqrt{\frac{\int_{t_5}^{t_{95}} a^2(t)\,\mathrm{d}t}{t_d}} \tag{4}$$

6) Characteristic intensity

$$I_c = a_{rms}^{1.5} t_d^{0.5} \tag{5}$$

7) Peak ground velocity

$$V_{PG} = \max | v(t) | \tag{6}$$

8) Sustained maximum velocity (V_{SM}): Third largest peak in velocity time history.

9) Specific energy density

$$I_{SED} = \int_0^{t_f} v^2(t)\,\mathrm{d}t \tag{7}$$

10) Velocity RMS

$$v_{rms} = \sqrt{\frac{\int_{t_5}^{t_{95}} v^2(t)\,\mathrm{d}t}{t_d}} \tag{8}$$

11) Compound velocity-related intensity measure

$$I_f = V_{PG} t_d^{0.25} \tag{9}$$

12) Peak ground displacement

$$D_{PG} = \max | d(t) | \tag{10}$$

13) Displacement squared integral

$$d_{sq} = \sqrt{\frac{\int_{t_5}^{t_{95}} d^2(t)\,\mathrm{d}t}{t_d}} \tag{11}$$

14) Displacement RMS

$$d_{rms} = \sqrt{\frac{\int_{t_5}^{t_{95}} d^2(t)\,\mathrm{d}t}{t_d}} \tag{12}$$

15) Composite displacement

$$I_d = D_{PG} t_d^{\frac{1}{3}} \tag{13}$$

16) Peak pseudo-spectrum acceleration

$$I_{PSA} = \max S_{pa} \tag{14}$$

17) Peak pseudo-spectrum velocity

$$I_{PSV} = \max S_{pv} \tag{15}$$

18) Acceleration spectrum intensity

$$I_{AS} = \int_{0.1}^{0.5} S_{pa}\,\mathrm{d}T \tag{16}$$

19) Velocity spectrum intensity

$$I_{VS} = \int_{0.1}^{0.5} S_{pv}\,\mathrm{d}T \tag{17}$$

20) Housner intensity

$$I_H = \int_{0.1}^{2.5} S_{pv}\,\mathrm{d}T \tag{18}$$

21) Effective peak acceleration

$$I_{EPA} = \frac{\int_{0.1}^{0.5} S_a\,\mathrm{d}T}{2.5} \tag{19}$$

where t_f is the total duration of the seismic motion; $a(t)$, $v(t)$ and $d(t)$ represent the acceleration, velocity, and displacement time histories, respectively; S_a, S_v, S_{pa}, and S_{pv} represent the spectral acceleration, the spectral velocity, the pseudo-spectral acceleration, and the pseudo-spectral velocity, respectively; t_5 and t_{95} represent the times at which 5% and 95% of the Arias intensity have been reached, respectively, and $t_d = t_{95} - t_5$ denotes the effective duration of strong earthquake shaking.

1.2 Evaluation criteria

The probabilistic seismic demand model is used to estimate the probability distribution of structural response under specific seismic intensity levels. This model establishes the relationship between IMs and the corresponding demands on different structures or components, facilitating an understanding of how different structures are likely to respond under various seismic conditions[13-14]. Cornell et al.[15] assumed that for a specific IM, the probability distribution of the damage measures (DMs) exceeding a specific demand level D follows a log-normal distribution as

$$\beta\{S_{DM} \geqslant D \mid S_{IM}\} = 1 - \Phi\left(\frac{\ln S_D - \ln D}{\beta_{tot}}\right) \tag{20}$$

where the probability of the S_{DM} exceeding a specific damage state D under a certain ground motion S_{IM} obeys a log-normal distribution, as shown in Eq. (20). Here, $\Phi(\cdot)$ represents the standard normal distribution function, S_D denotes the mean of the structural DM estimates, and β_{tot} presents the total log-normal standard deviation.

According to the research conducted by Cornell et al.[15], there exists a power-law correlation between S_D and S_{IM}:

$$S_D = aS_{IM}^b \tag{21}$$

By taking the natural logarithm of both sides of the above equation, the following expression is obtained as

$$\ln S_D = \ln a + b\ln S_{IM} \tag{22}$$

The evaluation criteria for selecting the optimal IMs mainly encompass four aspects: efficiency[16], practicality[17], proficiency[18], and sufficiency[19].

1.2.1 Efficiency

The efficiency of seismic motion intensity parameters is measured by the standard deviation of the logarithm of the residuals, denoted as β_D. For a specific IM, a smaller β_D indicates higher efficiency. The formula for β_D is shown as follows:

$$\beta_D = \sqrt{\frac{\sum [\ln d_i - \ln(aS_{IM}^b)]^2}{n-2}} \tag{23}$$

where d_i represents the i-th DMs obtained from the seismic analysis of the soil-structure interaction system.

1.2.2 Practicality

Practicality assesses whether there is a direct correlation between the DMs and the IM. This attribute can be measured using the regression parameter b in Eq. (22). A value of b close to zero suggests that the IM has negligible influence on DM, whereas a larger value of b denotes stronger practicality of that IM.

1.2.3 Proficiency

When evaluating seismic intensity measures using both efficiency and practicality criteria, different outcomes may arise. To address this, Padgett et al.[18] proposed a proficiency index as a primary criterion for selecting the seismic intensity measure. The proficiency index, denoted as ζ, considers both efficiency and practicality. Similar to efficiency, a smaller ζ indicates greater proficiency.

$$\zeta = \frac{\beta_D}{b} \tag{24}$$

1.2.4 Sufficiency

Sufficiency refers to the relative independence of a structure's response from seismic event parameters (such as earthquake magnitude M_w, fault distance R_{rup}) under a specific seismic intensity measure. Sufficiency can be evaluated by performing separate single-parameter linear regression analyses of the residuals ε with respect to M_w and R_{rup}. The regression equations can be expressed as follows:

$$\varepsilon_{IM} = \begin{cases} a_M + b_M M_W \\ a_R + b_R R_{rup} \end{cases} \tag{25}$$

To assess sufficiency, the P-value method is employed to test the hypothesis that the slope is equal to zero. The P-value is defined as the probability of erroneously rejecting the null hypothesis[19] in the regression analysis, assuming that the slope equals to zero. In this study, a significance level of 5% is used for the hypothesis test[19-20]. If the P-value exceeds 5%, the IM measure is generally considered to have sufficiency. A higher P-value for the slope indicates stronger evidence of the sufficiency of the IM measure.

2 Nonlinear Seismic Finite Element Model

2.1 Nonlinear beam-spring model considering tangential interaction

Previous models for foundation beams primarily addressed the longitudinal response of tunnels under full slip conditions, where the tangential interaction force is zero. This assumption highly idealizes the scenario, neglecting the crucial aspect of contact behavior between the tunnel lining and the surrounding medium. Recognizing this, our study adopts a modified beam-spring model proposed by Zhao et al.[21]. This model, as shown in Fig. 1, consists of a Timoshenko beam resting on Winkler foundation

springs and considers the tangential interaction through distributed equivalent bending moments acting on the beam. The tunnel beam has an outer diameter of 6.2 m, an inner diameter of 5.5 m, a lining thickness of 0.35 m, a length of 500 m, and a longitudinal steel reinforcement ratio of 1.24%, as shown in Fig. 1.

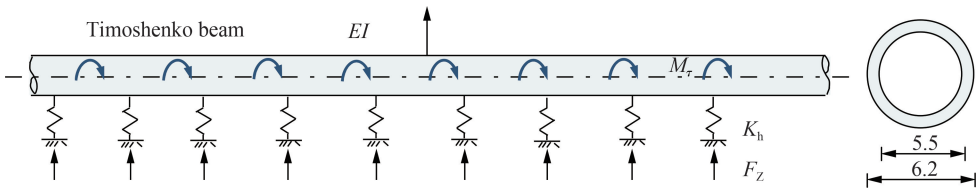

Fig. 1 Beam model on an elastic foundation (unit: m)

Nonlinear fiber elements are usually applied to expedite computational analysis. Specifically, this study utilizes the PQ-Fiber beam model[22] to simulate the nonlinear mechanical behavior of the reinforced concrete tunnel lining. Within this model, the concrete fibers are characterized by the UConcrete02 constitutive relationship, as shown in Fig. 2. Similarly, the steel fibers follow the USteel02 constitutive relationship, accommodating a motion hysteretic model, as indicated in Fig. 3. The constitutive parameters used for concrete and steel reinforcement are shown in Table 1.

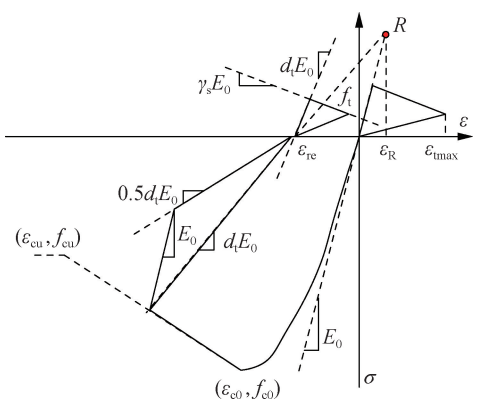

Fig. 2 Stress-strain relationship of concrete under uniaxial cyclic loading

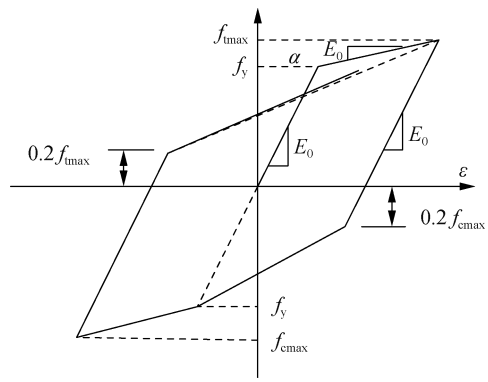

Fig. 3 Constitutive model considering the kinematic hardening elastic-plastic behavior of reinforcing steel

The incident seismic wave motion is converted into a distributed normal force F_z to account for the normal ground-tunnel interactions, which can be determined by

$$F_z = K_h u_g \tag{26}$$

where u_g represents the displacement of the incident seismic wave; K_h denotes the modulus of the Winkler foundation spring, as referred to in Zhao et al.[21], which can be given as

$$K_h = \frac{3E_g}{1-\nu_g^2}\left(\frac{E_g L}{2E_l R}\right)^{1/8} \tag{27}$$

Table 1 Material parameters for concrete and reinforcing steel

Material	Density ρ/(kg · m^{-3})	Elastic modulus E_g/GPa	Poisson's ratio ν	Yield strength f_y/MPa	Axial compressive strength f_{c0}/MPa	Peak compressive strain ε_{c0}	Ultimate compressive strain ε_{cu}
Steel	7 800	200.0	0.30	456			
Concrete	2 400	34.5	0.20		28	0.001 879	0.003 8

where E_g and ν_g indicate the elastic modulus and Poisson's ratio of the ground, respectively; E_l is the elastic modulus of the tunnel; L represents the wavelength; R and r are the outer and inner radius of the tunnel, respectively.

Moreover, the distributed moment M_τ is applied to the beam to consider the tangential ground-tunnel interactions, as referred to in Zhao et al.[21], which can be determined by

$$M_\tau = -K_2 \dot{u}_g \tag{28}$$

where $\dot{u}_g$ is the velocity of the incident seismic wave; K_2 is the tangential interaction coefficient, according to Zhao et al.[21], which can be expressed as

$$K_2 = \frac{2\pi G_g G_l (R^2 - r^2) R^3}{c_s R[G_g(R^2 + r^2) + G_l(R^2 - r^2)]} \tag{29}$$

where G_g and c_s are the shear modulus and shear velocity of the ground, respectively.

2.2 Site conditions

To account for the influence of ground conditions on the longitudinal seismic vulnerability of tunnels, five types of ground conditions were selected in this study by consulting the code for seismic design of urban rail transit structures (GB 50909—2014) and other references[23]. The ground conditions classified as Case Ⅰ to Ⅴ in this paper correspond to ground conditions Case $Ⅰ_0$, Case $Ⅰ_1$, Case Ⅱ, Case Ⅲ, and Case Ⅳ specified in the seismic design code. The mechanical parameters, including density ρ_g, elastic modulus E_g, shear wave velocity c_s, and Poisson's ratio ν_g, are listed in Table 2.

Table 2 Parameters of the surrounding ground

Ground cases	Density ρ_g/(kg·m^{-3})	Young's modulus E_g/MPa	Poisson's ratio ν_g	Shear velocity c_s/(m·s^{-1})
Case Ⅰ	2 000	54.0	0.35	100
Case Ⅱ	2 200	228.8	0.30	200
Case Ⅲ	2 400	877.5	0.30	375
Case Ⅳ	2 500	2 640.7	0.25	650
Case Ⅴ	2 600	6 500.0	0.25	1 000

2.3 Input ground motions

In this subsection, we selected a total of 50 pairs of horizontal seismic records from 24 different earthquake events sourced from the PEER website. Our selection was guided by the following criteria: 1) a moment magnitude (M_w) larger than 6; 2) the absence of velocity pulses. The pseudo-acceleration response spectra of these selected seismic records are displayed in Fig. 4. For the subsequent numerical analysis, each of the two horizontal components from every seismic record was individually input into the numerical model. Thus, this process resulted in a total of 100 numerical simulations.

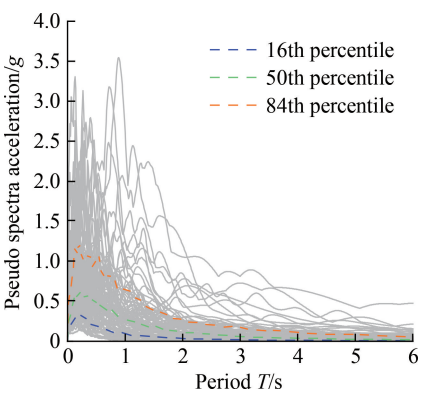

Fig. 4 Pseudo-acceleration response spectra

2.4 Damage measure

The DM is an important indicator to quantify structural damages when assessing seismic vulnerability. This work mainly focuses on selecting the optimal seismic intensity that influences the longitudinal seismic response of tunnels. For this purpose, a force-based DM has been selected, defined as the ratio of the actual bending moment M to the capacity bending moment M_{Rd} along the tunnel's longitudinal axis.

3 Evaluation of the Rationality of Seismic Intensity Measures

3.1 Efficiency testing

The efficiency testing results are presented in Fig. 5, focusing on the damage parameter of the peak bending moment ratio. Under softer soil conditions, the seismic velocity intensity measure emerges as the most effective. In both Case Ⅰ and Case Ⅱ, V_{SM} stands out as the most effective IM, with residual standard deviations β_D of 0.287 and 0.312, respectively. Conversely, I_{CAV} ranks as the least effective indicator, exhibiting residual standard deviations β_D of 0.601 and 0.618 for Cases Ⅰ and Ⅱ,

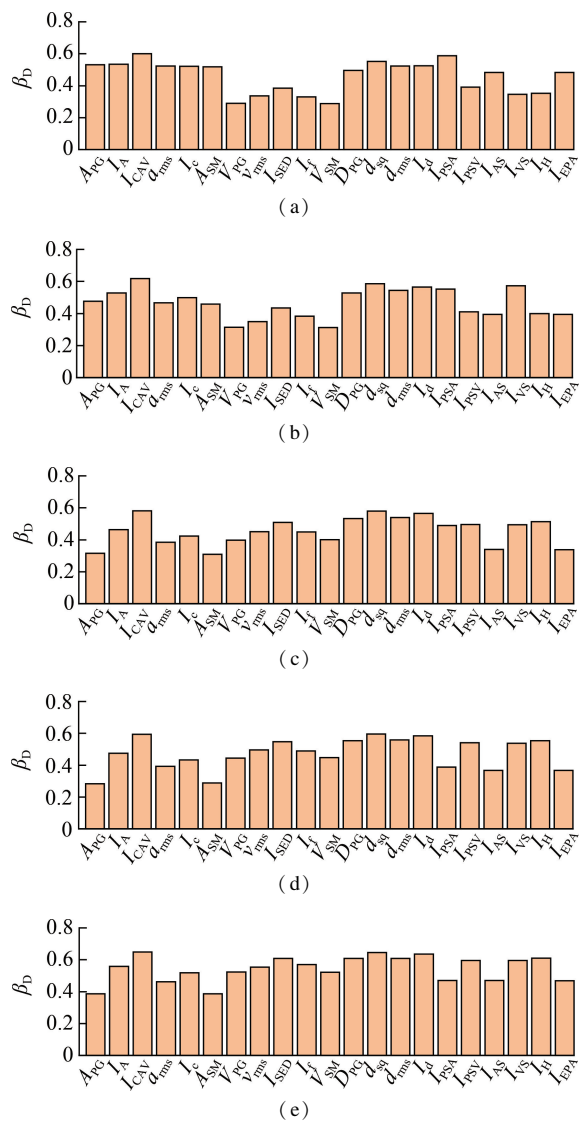

Fig. 5 Comparison of the effectiveness of seismic intensity parameters across different sites. (a) Case Ⅰ; (b) Case Ⅱ; (c) Case Ⅲ; (d) Case Ⅳ; (e) Case Ⅴ

respectively. As soil conditions gradually become stiffer, the seismic acceleration intensity measure is the most effective IM. In Cases Ⅲ and Ⅴ, A_{SM} proves to be the most efficient IM, with residual standard deviations β_D of 0.311 and 0.386, respectively. I_{CAV} remains the least effective IM, with residual standard deviations β_D of 0.581 and 0.649, respectively. In Case Ⅳ, A_{PG} is identified as the most effective IM, achieving the lowest residual standard deviation of 0.284, while the least effective IM is observed in d_{sq} with a residual standard deviation β_D of 0.596.

3.2 Practicality testing

The practicality results for each IM-DM pair, computed based on damage parameters related to the peak bending moment ratio, are summarized in Fig. 6. In the soft soil conditions of Case Ⅰ, the results in Fig. 6(a) indicate that V_{PG} is the most practical IM, exhibiting the largest slope b, specifically 0.801. As the soil gradually becomes stiffer, the practicality of the seismic acceleration intensity measure becomes more pronounced. The most practical seismic intensity measures across these cases are I_{AS}, I_{EPA}, A_{SM}, and A_{SM}, with corresponding slopes b of 0.927, 0.965, 1.002, and 0.954, respectively. Across all five soil conditions, d_{sq} is found to be the least practical IM, with corresponding slopes b of 0.168, 0.143, 0.135, 0.131, and 0.103.

3.3 Proficiency testing

Fig. 7 summarizes the calculated ζ values, which are used for assessing damage measures of the peak bending moment ratio. The most proficient IMs in both Case Ⅰ and Case Ⅱ are velocity-type seismic intensity measures. Specifically, V_{SM} and V_{PG} stand out with corresponding uncertainty parameters ζ of 0.359 and 0.412, respectively. In harder ground conditions, observed in Cases Ⅲ,

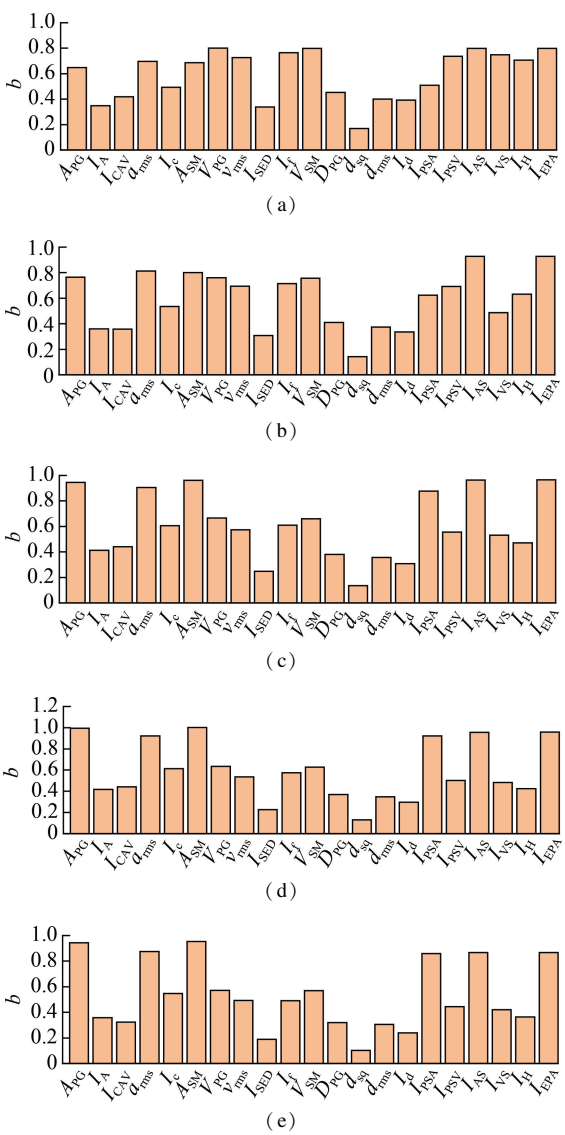

Fig. 6 Comparison of the practicality of seismic intensity parameters across different sites. (a) Case Ⅰ; (b) Case Ⅱ; (c) Case Ⅲ; (d) Case Ⅳ; (e) Case Ⅴ

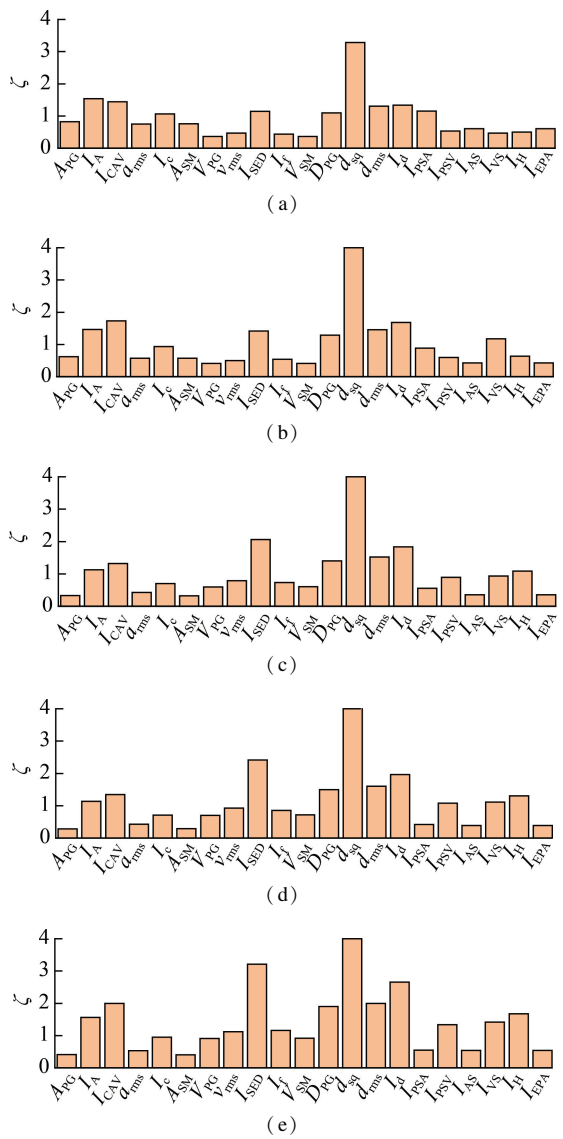

Fig. 7 Comparison of the proficiency properties of seismic intensity parameters across different sites. (a) Case Ⅰ; (b) Case Ⅱ; (c) Case Ⅲ; (d) Case Ⅳ; (e) Case Ⅴ

Ⅳ, and Ⅴ, the most proficient IMs shift to acceleration-type seismic intensity measures. In Cases Ⅲ and Ⅴ, A_{SM} is identified as the most proficient IM, featuring corresponding uncertainty parameters ζ of 0.322 and 0.404. In Case Ⅳ, A_{PG} is recognized as the most proficient IM, with an uncertainty parameter ζ of 0.285. Similar to findings on practicality, d_{sq} is found to be the least practical IM across all ground conditions, with significantly higher uncertainty parameters ζ of 3.284, 4.102, 4.302, 4.568, and 6.287.

3.4 Sufficiency testing

Table 3 presents the results of the conditional independence test regression models, analyzing the relationship between the residuals of the corresponding IM and DM in the longitudinal direction of a circular tunnel and both earthquake magnitude and distance. Based on Table 3, it is evident that all the *P*-values obtained from the regression analysis with earthquake magnitude exceeded 5%. This suggests a lack of correlation between the seismic intensity parameters and earthquake magnitude, thereby affirming the sufficiency evaluation based on earthquake magnitude.

3.5 Determining the optimal intensity parameters

The study investigated seismic intensity parameters

Table 3 Comparison of the sufficiency of seismic intensity parameters (peak bending moment ratio) in different sites

IM	*P*-value M_w					*P*-value R_{rup}				
	Case Ⅰ	Case Ⅱ	Case Ⅲ	Case Ⅳ	Case Ⅴ	Case Ⅰ	Case Ⅱ	Case Ⅲ	Case Ⅳ	Case Ⅴ
A_{PG}	0.386	0.411	0.478	0.504	0.526	0.610	0.585	0.516	0.476	0.502
I_A	0.487	0.487	0.568	0.583	0.591	0.654	0.602	0.546	0.521	0.609
I_{CAV}	0.469	0.466	0.532	0.543	0.531	0.722	0.598	0.550	0.530	0.680
a_{rms}	0.409	0.425	0.496	0.515	0.542	0.604	0.585	0.515	0.486	0.522
I_c	0.470	0.476	0.558	0.575	0.592	0.630	0.599	0.538	0.511	0.576
A_{SM}	0.391	0.414	0.486	0.513	0.533	0.604	0.582	0.508	0.467	0.491
V_{PG}	0.542	0.463	0.532	0.540	0.571	0.534	0.537	0.462	0.444	0.533
v_{rms}	0.539	0.463	0.520	0.527	0.561	0.574	0.578	0.499	0.479	0.560
I_{SED}	0.618	0.519	0.549	0.550	0.565	0.658	0.594	0.521	0.501	0.617
I_f	0.614	0.513	0.559	0.562	0.580	0.607	0.559	0.488	0.469	0.581
V_{SM}	0.545	0.464	0.531	0.539	0.571	0.532	0.537	0.462	0.445	0.532
D_{PG}	0.527	0.468	0.518	0.528	0.562	0.710	0.626	0.560	0.537	0.650
d_{sq}	0.505	0.463	0.511	0.520	0.533	0.745	0.621	0.563	0.541	0.679
d_{rms}	0.496	0.453	0.505	0.516	0.552	0.713	0.629	0.566	0.543	0.653
I_d	0.528	0.473	0.520	0.528	0.544	0.737	0.621	0.559	0.537	0.671
I_{PSA}	0.396	0.430	0.501	0.520	0.534	0.657	0.585	0.530	0.541	0.573
I_{PSV}	0.518	0.483	0.525	0.528	0.538	0.599	0.548	0.488	0.474	0.586
I_{AS}	0.417	0.454	0.541	0.556	0.540	0.580	0.552	0.462	0.435	0.504
I_{VS}	0.533	0.499	0.533	0.535	0.535	0.561	0.527	0.476	0.463	0.576
I_H	0.545	0.498	0.528	0.530	0.530	0.577	0.535	0.484	0.470	0.589
I_{EPA}	0.417	0.454	0.541	0.556	0.540	0.580	0.552	0.462	0.435	0.504

suitable for assessing the seismic performance of subway stations subjected to seismic activity. Table 4 summarizes the most effective, practical, and proficient seismic intensity parameters for tunnel structures across five different site conditions. The findings reveal that as site conditions shift from soft to hard, the proficiency of velocity-based seismic intensity parameters gradually decreases, while the effectiveness of acceleration-based seismic intensity parameters gradually increases.

Table 4 Optimal intensity parameters in different site conditions

Evaluation criteria	Case Ⅰ	Case Ⅱ	Case Ⅲ	Case Ⅳ	Case Ⅴ
Efficiency	V_{SM}	V_{SM}	A_{SM}	A_{PG}	A_{SM}
Practicality	V_{PG}	I_{AS}	I_{EPA}	A_{SM}	A_{SM}
Proficiency	V_{SM}	V_{PG}	A_{SM}	A_{PG}	A_{SM}

4 Conclusions

1) The proficiency of acceleration-related IMs tends to decrease with softer site conditions, while the proficiency of velocity-related IMs increases. In addition, displacement-related IMs show inferior performance compared to other types of IMs based on the proficiency criterion.

2) Site conditions significantly influence the determination of optimal IMs. Considering the criteria of efficiency, practicality, proficiency, and sufficiency, V_{SM} emerges as the optimal IM for circular tunnels in site Case Ⅰ, V_{PG} is deemed optimal for site Case Ⅱ, A_{SM} is the optimal IM for site Cases Ⅲ and Ⅴ, and PGA stands out as the optimal IM for site Case Ⅳ.

3) Among the three commonly used amplitude intensity parameters (A_{PG}, V_{PG}, D_{PG}), V_{PG} is found to be suitable for site Cases Ⅰ and Ⅱ, while A_{PG} fits site Cases Ⅲ, Ⅳ, and Ⅴ better.

4) In this study, the evaluation of structural damage indicators is limited to force-based, non-cumulative dam-

age parameters. Subsequent research should consider energy-based, cumulative damage parameters, which could better reflect tunnel damage. Additionally, seismic responses of tunnel structures are influenced by factors such as structural burial depth and the ratio of structural soil/rock flexibility. Further investigation into these factors is necessary to derive more universal conclusions.

References

[1] He C, Koizumi A. Study on seismic behavior and seismic design methods in transverse direction of shield tunnels[J]. *Structural Engineering and Mechanics*, 2001, **11**(6): 651 - 662. DOI: 10.12989/sem.2001.11.6.651.

[2] Liu X D, Liu M H, Jin X N. Technological development and prospect of China's large-scale cross-sea passage project[J]. *Journal of Southeast University* (*Natural Science Edition*), 2023, **53**(6): 988 - 996. DOI: 10.3969/j.issn.1001-0505.2023.06.005. (in Chinese)

[3] Huang Z K, Pitilakis K, Tsinidis G, et al. Seismic vulnerability of circular tunnels in soft soil deposits: The case of Shanghai metropolitan system[J]. *Tunnelling and Underground Space Technology*, 2020, **98**: 103341. DOI: 10.1016/j.tust.2020.103341.

[4] Liu H Q, Song K Z, Ye Z, et al. Seismic fragility analysis of in-service shield tunnels considering surface building and joint-bolt corrosion[J]. *Soil Dynamics and Earthquake Engineering*, 2022, **162**: 107455. DOI: 10.1016/j.soildyn.2022.107455.

[5] Wang M, Du X L, Sun F F, et al. Fragility analysis and inelastic seismic performance of steel braced-core-tube frame outrigger tall buildings with passive adaptive negative stiffness damped outrigger[J]. *Journal of Building Engineering*, 2022, **52**: 104428. DOI: 10.1016/j.jobe.2022.104428.

[6] Yu X H, Zhou Z, Du W Q, et al. Development of fragility surfaces for reinforced concrete buildings under mainshock-aftershock sequences[J]. *Earthquake Engineering & Structural Dynamics*, 2021, **50**(15): 3981 - 4000. DOI: 10.1002/eqe.3542.

[7] Lin J C, Sun W Y, Li G Y, et al. Seismic fragility of shallowly buried bias loess tunnels based on vector-valued intensity measures[J]. *Journal of Southeast University* (*Natural Science Edition*), 2024, **54**(2): 432 - 440. DOI: 10.3969/j.issn.1001-0505.2024.02.021. (in Chinese)

[8] Chen Z Y, Wei J S. Correlation between ground motion parameters and lining damage indices for mountain tunnels[J]. *Natural Hazards*, 2013, **65**(3): 1683 - 1702. DOI: 10.1007/s11069-012-0437-5.

[9] Zhang C M, Zhong Z L, Zhao M. Study on ground motion intensity measures for seismic response evaluation of circular tunnel[J]. *IOP Conference Series: Earth and Environmental Science*, 2020, **455**(1): 012164. DOI: 10.1088/1755-1315/455/1/012164.

[10] Hashash Y M A, Park D. Non-linear one-dimensional seismic ground motion propagation in the Mississippi embayment[J]. *Engineering Geology*, 2001, **62**(1/2/3): 185 - 206. DOI: 10.1016/S0013-7952(01)00061-8.

[11] Jiang B J, Xian Q L, Zhou F L. The influence analysis of the effect of pile-soil contact on the seismic response of the high speed railway bridge[J]. *Journal of Guangzhou University* (*Natural Science Edition*), 2016, **15**(1): 57 - 63. (in Chinese)

[12] Shakib H, Jahangiri V. Intensity measures for the assessment of the seismic response of buried steel pipelines[J]. *Bulletin of Earthquake Engineering*, 2016, **14**(4): 1265 - 1284. DOI: 10.1007/s10518-015-9863-6.

[13] Jiang H, Gu Q, Huang L, et al. Analysis on seismic vulnerability of offshore cable-stayed bridge considering time-dependent deterioration by chloride-induced corrosion[J]. *Journal of Southeast University* (*Natural Science Edition*), 2021, **51**(1): 38 - 45. DOI: 10.3969/j.issn.1001-0505.2021.01.006. (in Chinese)

[14] Jiang H, Li C, Feng M Y, et al. Analysis on probabilistic seismic damage characteristics of dry joint prefabricated bridge pier based on kernel density estimation[J]. *Journal of Southeast University* (*Natural Science Edition*), 2021, **51**(4): 566 - 574. DOI: 10.3969/j.issn.1001-0505.2021.04.003. (in Chinese)

[15] Cornell C A, Jalayer F, Hamburger R O, et al. Probabilistic basis for 2000 SAC federal emergency management agency steel moment frame guidelines[J]. *Journal of Structural Engineering*, 2002, **128**(4): 526 - 533. DOI: 10.1061/(asce)0733-9445(2002)128: 4(526).

[16] Deng X S, Lai X Y, Yuan K, et al. Vulnerability analysis of multiple ground motion intensity measure rectors for high-rise RC frame structure under rare earthquake[J]. *World Earthquake Engineering*, 2022, **38**(3): 19 - 29. DOI: 10.19994/j.cnki.WEE.2022.0053. (in Chinese)

[17] Mackie K, Stojadinović B. Probabilistic seismic demand model for California highway bridges[J]. *Journal of Bridge Engineering*, 2001, **6**(6): 468 - 481. DOI: 10.1061/(asce)1084-0702(2001)6: 6(468).

[18] Padgett J E, Nielson B G, DesRoches R. Selection of optimal intensity measures in probabilistic seismic demand models of highway bridge portfolios[J]. *Earthquake Engineering & Structural Dynamics*, 2008, **37**(5): 711 - 725. DOI: 10.1002/eqe.782.

[19] Luco N, Cornell C A. Structure-specific scalar intensity measures for near-source and ordinary earthquake ground motions[J]. *Earthquake Spectra*, 2007, **23**(2): 357 - 392. DOI: 10.1193/1.2723158.

[20] Tsinidis G, Di Sarno L, Sextos A, et al. Optimal intensity measures for the structural assessment of buried steel natural gas pipelines due to seismically-induced axial compression at geotechnical discontinuities[J]. *Soil Dynamics and Earthquake Engineering*, 2020, **131**: 106030. DOI: 10.1016/j.soildyn.2019.106030.

[21] Zhao M, Li H F, Huang J Q, et al. Analytical solutions considering tangential contact conditions for circular lined tunnels under longitudinally propagating shear waves[J]. *Computers and Geotechnics*, 2021, **137**: 104301. DOI: 10.1016/j.compgeo.2021.104301.

[22] Liu Z Q, Du Z Y, Xue J Y, et al. Experimental study and finite element analysis on seismic behavior of solid-web steel reinforced concrete cross-shaped and L-shaped columns[J]. *Journal of Building Structures*, 2019, **40**(4): 104 - 115. DOI: 10.14006/j.jzjgxb.2019.04.

011. (in Chinese)
[23] Li X Y, Zhao X, Li Y H. Green's functions of the forced vibration of Timoshenko beams with damping effect[J]. *Journal of Sound and Vibration*, 2014, **333**(6): 1781 – 1795. DOI: 10.1016/j.jsv.2013.11.007.

适用于隧道纵向地震响应评估的地震动强度参数优选

赵 旭[1] 杨宇杰[1] 黄景琦[2] 赵 密[1] 曹胜涛[3]

([1] 北京工业大学城市安全与灾害工程教育部重点实验室, 北京 100124)
([2] 北京科技大学土木与资源工程学院, 北京 100083)
([3] 广州颖力科技有限公司, 广州 510700)

摘要:为研究适用于隧道结构纵向抗震性能设计的地震动强度参数(IMs),选取21个不同的地震动强度参数进行了隧道结构的非线性计算和分析,以确定不同场地条件下隧道结构纵向的最优IM. 建立了改进非线性梁–弹簧模型以计算隧道结构纵向的地震响应,其中采用了PQ-Fiber模型来模拟隧道结构纵向的非线性行为,以弯矩荷载作用在隧道结构上的形式模拟隧道与土之间的切向相互作用;选取了5种不同的场地类型,采用有效性、实用性、有益性和充分性4类评价准则对21个IMs进行优选. 结果表明:场地条件对最佳IMs具有显著影响,持续最大速度V_{SM}是Ⅰ级场地圆形隧道的最佳IM;峰值速度V_{PG}是Ⅱ级场地的最佳IM;持续最大加速度A_{SM}是Ⅲ级和Ⅴ级场地的最佳IM;峰值加速度A_{PG}是Ⅳ级场地的最佳IM. 可见,随着场地条件从Ⅰ类到Ⅴ类,从软到硬,加速度型强度参数适用性逐渐降低,而速度型强度参数适用性逐渐增强.

关键词:地震动强度参数;隧道纵向;概率性地震需求模型;土–结相互作用;改进地基–梁模型
中图分类号:TU921